

Theory of magnon-driven spin Seebeck effect

Jiang Xiao (萧江)^{1,2}, Gerrit E. W. Bauer², Ken-ichi Uchida^{3,4}, Eiji Saitoh^{3,4,5}, and Sadamichi Maekawa^{3,6}

¹*Department of Physics and State Key Laboratory of Surface Physics, Fudan University, Shanghai 200433, China*

²*Kavli Institute of NanoScience, Delft University of Technology, 2628 CJ Delft, The Netherlands*

³*Institute for Materials Research, Tohoku University, Sendai 980-8557, Japan*

⁴*Department of Applied Physics and Physico-Informatics, Keio University, Yokohama 223-8522, Japan*

⁵*PRESTO, Japan Science and Technology Agency, Sanbancho, Tokyo 102-0075, Japan*

⁶*CREST, Japan Science and Technology Agency, Tokyo 100-0075, Japan*

(Dated: September 7, 2010)

The spin Seebeck effect is a spin-motive force generated by a temperature gradient in a ferromagnet that can be detected via normal metal contacts through the inverse spin Hall effect [K. Uchida *et al.*, Nature **455**, 778-781 (2008)]. We explain this effect by spin pumping at the contact that is proportional to the spin-mixing conductance of the interface, the inverse of a temperature-dependent magnetic coherence volume, and the difference between the magnon temperature in the ferromagnet and the electron temperature in the normal metal [D. J. Sanders and D. Walton, Phys. Rev. B **15**, 1489 (1977)].

I. INTRODUCTION

The emerging field called *spin caloritronics* addresses charge and heat flow in spin-polarized materials, structures, and devices. Most thermoelectric phenomena can depend on spin, as discussed by many authors in Ref. 1. A recent and not yet fully explained experiment² is the spin analogue of the Seebeck effect — the spin Seebeck effect, in which a temperature gradient over a ferromagnet gives rise to an inverse spin Hall voltage signal in an attached Pt electrode.

The Seebeck effect refers to the electrical current/voltage that is induced when a temperature bias is applied across a conductor. By connecting two conductors with different Seebeck coefficients electrically at one end at a certain temperature, a voltage can be measured between the other two ends when kept at a different temperature. The spin counterpart of such a thermocouple is the spin current/accumulation that is induced by a temperature difference applied across a ferromagnet, interpreting the two spin channels as the two “conductors”. In Uchida *et al.*’s experiment,² a temperature bias is applied over a strip of a ferromagnetic film. A thermally induced spin signal is measured by the voltage induced by the inverse spin Hall effect (ISHE)^{3,4} in Pt contacts on top of the film in transverse direction (see Fig. 1). This Hall voltage is found to be approximately a linear function (possibly a hyperbolic function with long decay length) of the position in longitudinal direction over a length of several millimeters. This result has been puzzling, since spin-dependent length scales are usually much smaller. The original explanation for this experiment has been based on the thermally induced spin accumulation in terms of the spin thermocouple analogue mentioned above. However, the spin flip scattering short-circuits the spin channels, and at which spin channels are short-circuited, the signal should vanish on the scale of the spin-flip diffusion length.⁵

In this paper, we propose an alternative mechanism in terms of spin pumping caused by the difference between the magnon temperature in the ferromagnetic film and the electron temperature (assumed equal to the phonon temperature) in the Pt contact. Such a temperature difference can be generated by a temperature bias applied over the ferromagnetic film.⁶

This paper is organized as follows: Section II describes how a DC spin current is pumped through a ferromagnet(F)|normal metal(N) interface by a difference between the magnon temperature in F and electron temperature in N. In section III we calculate the magnon temperature profile in F under a temperature bias. In Section IV we compute the thermally driven spin current as a function of the position of the normal metal contact.

II. THERMALLY DRIVEN SPIN PUMPING CURRENT ACROSS F|N INTERFACE

In this Section we derive expressions for the spin current flowing through an F|N interface with a temperature difference as shown in Fig. 2, starting with the macrospin approximation in Subsection II.A and considering finite magnon dispersion in Subsection II.B.

Since the relaxation times in the spin, phonon, and electron subsystems are much shorter than the spin-lattice relaxation time,^{7,13} the reservoirs become thermalized internally before they equilibrate with each other. Therefore, we may assume that the phonon (p), conduction electron (e), and magnon (m) subsystems can be described by their local temperatures: $T_F^{p,e,m}$ in F, and $T_N^{p,e}$ in N.⁸ We furthermore assume that the electron-phonon interaction is strong enough such that locally $T_F^p = T_F^e \equiv T_F$ and $T_N^p = T_N^e \equiv T_N$. However, the magnon temperature may deviate: $T_F^m \neq T_F$. This is illustrated below by the extreme case of the macrospin model, in which there is only one constant magnetic temperature, whereas the electron and phonon temperatures linearly interpolate between the reservoir temperatures T_L and T_R . The difference between magnon and electron/phonon temperature therefore changes sign in the center of the sample. When considering ferromagnetic insulators, the conduction electron subsystem in F becomes irrelevant.

A. F|N contact

First, let us consider a structure such as shown in Fig. 2, in which the magnetization is a single domain and can be regarded as a macrospin $\mathbf{M} = M_s V \mathbf{m}$, where \mathbf{m} is the unit vector parallel to the magnetization. We will derive in Subsection II.B the criteria for the macrospin regime. We assume uniaxial anisotropy along $\hat{\mathbf{z}}$, M_s is the saturation magnetization and V is the total F volume. The macrospin assumption will be relaxed below,

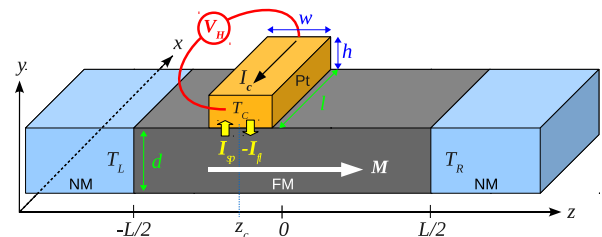


FIG. 1. (Color online) A ferromagnet (F) with thickness d and length L and magnetization \mathbf{M} pointing in $\hat{\mathbf{z}}$ -direction connects two normal metal (N) contacts at temperature $T_{L/R}$ at the left and right ends. A Pt strip of dimension $l \times w \times h$ on top of F converts an injected spin current ($\mathbf{I}_s = \mathbf{I}_{sp} + \mathbf{I}_{fl}$) into an electrical current I_c or Hall voltage V_H by the inverse spin Hall effect.

but serves to illustrate the basic physics.

At finite temperature the magnetization order parameter in F is thermally activated, *i.e.* $\dot{\mathbf{m}} \neq 0$. When we assume N to be an ideal reservoir, a spin current noise \mathbf{I}_{sp} is emitted into N due to spin pumping according to:⁹

$$\mathbf{I}_{sp}(t) = \frac{\hbar}{4\pi} [g_r \mathbf{m}(t) \times \dot{\mathbf{m}}(t) + g_i \dot{\mathbf{m}}(t)], \quad (1)$$

where g_r and g_i are the real and imaginary part of the spin-mixing conductance $g_{\text{mix}} = g_r + ig_i$ of the F|N interface. The thermally activated magnetization dynamics is determined by the magnon temperature T_F^m , while the lattice and electron temperatures are $T_F^p = T_F^e = T_F$. The term proportional to g_r in \mathbf{I}_{sp} has the same form as the magnetic damping phenomenology of the Landau-Lifshitz Gilbert equation (introduced below in Eq. (6)). The energy loss due to the spin current represented by g_r therefore increases the Gilbert damping constant. According to the Fluctuation-Dissipation Theorem (FDT), the noise component of this spin-pumping induced current (from F to N) is accompanied by a fluctuating spin current \mathbf{I}_{fl} from the normal metal bath (from N to F). The latter is caused by the thermal noise in N and its effect on F can be described by a random magnetic field \mathbf{h}' acting on the magnetization:¹⁰

$$\mathbf{I}_{fl}(t) = -\frac{M_s V}{\gamma} \mathbf{m}(t) \times \mathbf{h}'(t). \quad (2)$$

In the classical limit (at high temperatures $k_B T \gg \hbar \omega_0$, where ω_0 is the ferromagnetic resonance frequency) $\mathbf{h}'(t)$ satisfies the time correlation

$$\langle \gamma h'_i(t) \gamma h'_j(0) \rangle = \frac{2\alpha' \gamma k_B T_N}{M_s V} \delta_{ij} \delta(t) \equiv \sigma'^2 \delta_{ij} \delta(t). \quad (3)$$

where $\langle \dots \rangle$ denotes the ensemble average, $i, j = x, y$, and $\alpha' = (\gamma \hbar / 4\pi M_s V) g_r$ is the magnetization damping contribution caused by the spin pumping. The correlator is proportional to the temperature T_N .

The spin current flowing through the interface is given by the sum $\mathbf{I}_s = \mathbf{I}_{sp} + \mathbf{I}_{fl}$ (see Fig. 2). Here we are interested in the DC component:

$$\langle \mathbf{I}_s \rangle = \frac{M_s V}{\gamma} [\alpha' \langle \mathbf{m} \times \dot{\mathbf{m}} \rangle + \gamma \langle \mathbf{m} \times \mathbf{h}' \rangle], \quad (4)$$

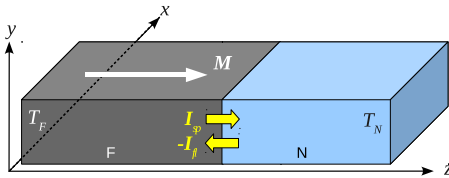


FIG. 2. (Color online) F|N interface with 1) spin pumping current \mathbf{I}_{sp} driven by the thermal activation of the magnetization in F at temperature T_F , and 2) fluctuating spin current \mathbf{I}_{fl} driven by the thermal activation of the electron spins in N at temperature T_N .

At thermal equilibrium, $T_N = T_F^m$, and $\langle \mathbf{I}_s \rangle = 0$. At non-equilibrium situation, the spin current component polarized along $\dot{\mathbf{m}}$ with prefactor g_i in Eq. (1) averages to zero, thus does not cause observable effects on the DC properties in the present model. The $\hat{\mathbf{x}}$ and $\hat{\mathbf{y}}$ component of $\langle \mathbf{I}_s \rangle$ also vanish and:

$$\langle I_z \rangle = \frac{M_s V}{\gamma} [\alpha' \langle m_x \dot{m}_y - m_y \dot{m}_x \rangle - \gamma \langle m_x h'_y - m_y h'_x \rangle]. \quad (5)$$

We therefore have to evaluate the correlators: $\langle m_i(0) \dot{m}_j(0) \rangle$ and $\langle m_i(0) h'_j(0) \rangle$.

The motion of \mathbf{m} is governed by the Landau-Lifshitz-Gilbert (LLG) equation:

$$\dot{\mathbf{m}} = -\gamma \mathbf{m} \times (H_{\text{eff}} \hat{\mathbf{z}} + \mathbf{h}) + \alpha \mathbf{m} \times \dot{\mathbf{m}}, \quad (6)$$

where H_{eff} and α are the effective magnetic field and total magnetic damping, respectively. \mathbf{h} accounts for the random fields associated with all sources of magnetic damping, *viz.* thermal random field \mathbf{h}_0 from the lattice associated with the bulk damping α_0 , random field \mathbf{h}' from the N contact associated with enhanced damping α' , and possibly other random fields caused by, *e. g.* additional contacts. Random fields from unrelated noise sources are statistically independent. The correlators of \mathbf{h} are therefore additive and determined by the total magnetic damping $\alpha = \alpha_0 + \alpha' + \dots$:

$$\langle \gamma h_i(t) \gamma h_j(0) \rangle = \frac{2\alpha \gamma k_B T_F^m}{M_s V} \delta_{ij} \delta(t) \equiv \sigma^2 \delta_{ij} \delta(t). \quad (7)$$

The magnon temperature T_F^m is affected by the temperatures of and couplings to all subsystems: $\alpha T_F^m = \alpha_0 T_F + \alpha' T_N + \dots$.

We consider near-equilibrium situations, thus we may linearize the LLG equation. To first order in $m_\perp \ll 1$ (with $m_z \simeq 1$)

$$\dot{m}_x + \alpha \dot{m}_y = -\omega_0 m_y + \gamma h_y, \quad (8a)$$

$$\dot{m}_y - \alpha \dot{m}_x = +\omega_0 m_x - \gamma h_x, \quad (8b)$$

where $\omega_0 = \gamma H_{\text{eff}}$ is the ferromagnetic resonance (FR) frequency. With the Fourier transform into frequency space $\tilde{g} = \int g e^{i\omega t} dt$ and the inverse transform $g = \int \tilde{g} e^{-i\omega t} d\omega / 2\pi$, Eq. (8) reads $\tilde{m}_i(\omega) = \sum_j \chi_{ij}(\omega) \gamma \tilde{h}_j(\omega)$, with $i, j = x, y$ and the transverse dynamic magnetic susceptibility

$$\chi(\omega) = \frac{1}{(\omega_0 - i\alpha\omega)^2 - \omega^2} \begin{pmatrix} \omega_0 - i\alpha\omega & -i\omega \\ i\omega & \omega_0 - i\alpha\omega \end{pmatrix}, \quad (9)$$

in terms of which, utilizing Eqs. (3, 7),

$$\langle m_i(t) m_j(0) \rangle = \frac{\sigma^2}{2\alpha} \int \frac{\chi_{ij}(\omega) - \chi_{ji}^*(\omega)}{i\omega} e^{-i\omega t} \frac{d\omega}{2\pi}, \quad (10a)$$

$$\langle m_i(t) h'_j(0) \rangle = \frac{\sigma'^2}{\gamma} \int \chi_{ij}(\omega) e^{-i\omega t} \frac{d\omega}{2\pi}. \quad (10b)$$

Eq. (10a) gives the mean square deviation of \mathbf{m} in the equal time limit $t \rightarrow 0$: $\langle m_i(0)m_j(0) \rangle = \delta_{ij}\gamma k_B T_F^m / \omega_0 M_s V$. The time derivative of Eq. (10a) is

$$\langle \dot{m}_i(t)m_j(0) \rangle = -\frac{\sigma^2}{2\alpha} \int [\chi_{ij}(\omega) - \chi_{ji}^*(\omega)] e^{-i\omega t} \frac{d\omega}{2\pi}, \quad (11)$$

By inserting Eqs. (10b, 11) with $t \rightarrow 0$ into Eq. (5):

$$\begin{aligned} \langle I_z \rangle &= \frac{M_s V}{\gamma} \left(\frac{\alpha'}{\alpha} \sigma^2 - \sigma'^2 \right) \int [\chi_{xy}(\omega) - \chi_{yx}(\omega)] \frac{d\omega}{2\pi} \\ &= \frac{2\alpha' k_B}{1 + \alpha^2} (T_F^m - T_N) \simeq \frac{\gamma \hbar g_r k_B}{2\pi M_s V} (T_F^m - T_N) \\ &\equiv L'_s (T_F^m - T_N), \end{aligned} \quad (12)$$

where L'_s is an interfacial spin Seebeck coefficient. In Eq. (12), we used $\int \text{Im}[\chi_{ij}(\omega)] d\omega / 2\pi = 0$ (since Eq. (10b) is real and $\text{Im}\chi$ changes sign when $\omega \rightarrow -\omega$), and $\int [\chi_{xy}(\omega) - \chi_{yx}(\omega)] (d\omega / 2\pi) = 1 / (1 + \alpha^2)$ (see Appendix A). From Eq. (12) we conclude that the DC spin pumping current is proportional to the temperature difference between the magnon and electron/lattice temperatures and polarized along the average magnetization.

When the magnon temperature is higher (lower) than the lattice temperature, the DC spin pumping current flows from F into N leading to a loss (gain) of angular momentum that is accompanied by the heat current:

$$Q_m = \frac{2\mu_B}{\hbar} \langle I_z \rangle H_{\text{eff}} = K'_m A (T_F^m - T_N), \quad (13)$$

where A is the contact area and $K'_m = \omega_0 \mu_B k_B (g_r / A) / \pi M_s V$ is the interface magnetic heat conductance with Bohr magneton μ_B .

In addition to the DC component of the spin pumping current, there is also an AC contribution to the frequency power spectrum of spin current and spin Hall signal.¹¹ A measurement of the noise power spectrum should be interesting for insulating ferromagnets for which the large imaginary part of the mixing conductance can be much larger than the real part (see Appendix B).

B. Magnons

In extended ferromagnetic layers the macrospin model breaks down and we have to consider magnon excitations at all wave vectors. The space-time magnetization autocorrelation function can be derived from the LLG equation (see Appendix C):

$$\langle \dot{m}_i(0,0)m_i(0,0) \rangle = \frac{\gamma k_B T_F^m}{M_s V_a}, \quad (14)$$

where we introduced the temperature-dependent magnetic coherence volume

$$V_a = \frac{2}{3Z_{\frac{5}{2}}} \left(\frac{4\pi D}{k_B T_F^m} \right)^{\frac{3}{2}} \quad (15)$$

with D the spin stiffness, and Z the Zeta function. Physically, this coherence volume, or its cube root, the coherence length, reflects the finite stiffness of the magnetic systems that limits the range at which a given perturbation is felt. When this length is small, a random field has a larger effect on a smaller magnetic volume.

The results obtained in Subsection II.A can be carried over simply by replacing $V \rightarrow V_a$ in Eqs. (3-7). The corresponding spin Seebeck coefficient is $L'_s = \gamma \hbar k_B (g_r / A) / 2\pi M_s V_a$, and the heat conductance is $K'_m = \omega_0 \mu_B k_B (g_r / A) / \pi M_s V_a$. Here we assumed that the magnon temperature does not change appreciably in the volume $V_a \ll V$.

III. MAGNON-PHONON TEMPERATURE DIFFERENCE PROFILE

Sanders and Walton (SW)⁶ discussed a scenario in which a magnon-phonon temperature difference arises when a constant heat flow (or a temperature gradient) is applied over an F insulator with special attention to the ferrimagnet yttrium iron garnet (YIG). Its antiferromagnetic component is small and will be disregarded in the following. This material is especially interesting because of its small Gilbert damping, which translates into a long length scale of persistence of a non-equilibrium state between the magnetic and lattice systems. SW assumes that, at the boundaries heat can only penetrate through the phonon subsystem, whereas magnons can not communicate with the non-magnetic heat baths (*i.e.* $K'_m = 0$ in our notation). Inside F bulk magnons interact with phonons and become gradually thermalized with increasing distance from the interface. The different boundary conditions for phonons and magnons lead to different phonon and magnon temperature profiles within F. However, according to Eq. (13), the magnons in F are not completely insulated as assumed by SW when the heat reservoirs are normal metals. In this section, we follow SW and calculate the phonon-magnon temperature difference in an F insulator film induced by the temperature bias but consider also the magnon thermal conductivity K'_m of the interfaces. In case of a metallic ferromagnet the conduction electron system provides an additional parallel channel for the heat current.

As argued above, the boundary conditions employed by SW need to be modified when the heat baths connected to the ferromagnet are metals. In that case, the magnons are not fully confined to the ferromagnet, since a spin current can be pumped into or extracted out of the normal metal. In Fig. 1, the two ends of F are at different temperatures: T_L and T_R of the N contacts drive the heat flow. Let us ignore the Pt contact on top of the F for now. When both phonons and magnons are in contact with the reservoirs, by energy conservation (similar to Ref. 6) the integrated heat Q_{mp} (\dot{Q}_{mp}) flowing from the phonon to the magnon subsystem in the range of $-L/2 \leq z' \leq z$ ($z \leq z' \leq L/2$) has the following form:

$$Q_{mp}(z) = \frac{C_p C_m}{C_T} \frac{1}{\tau_{mp}} \int_{-\frac{L}{2}}^z [T_p(z') - T_m(z')] dz' \quad (16a)$$

$$= +K_m \frac{dT_m}{dz} + K'_m [T_m(-L/2) - T_L] \quad (16b)$$

$$= -K_p \frac{dT_p}{dz} - K'_p [T_p(-L/2) - T_L], \quad (16c)$$

$$\bar{Q}_{mp}(z) = \frac{C_p C_m}{C_T} \frac{1}{\tau_{mp}} \int_z^{\frac{L}{2}} [T_p(z') - T_m(z')] dz' \quad (16d)$$

$$= -K_m \frac{dT_m}{dz} + K'_m [T_m(L/2) - T_R] \quad (16e)$$

$$= +K_p \frac{dT_p}{dz} - K'_p [T_p(L/2) - T_R], \quad (16f)$$

where $C_{p,m}$ ($C_T = C_p + C_m$) are the specific heats, $K_{p,m}$ ($K_T = K_p + K_m$) are the bulk thermal conductivities for the phonon and magnon subsystems, $K'_{p,m}$ ($K'_T = K'_p + K'_m$) are the respective boundary thermal conductivities. τ_{mp} is the magnon-phonon thermalization (or spin-lattice relaxation) time.⁷ The boundary conditions for T_m and T_p are set by letting $z = \pm L/2$ in Eq. (16), *i.e.*

$$K_{m,p} \frac{dT_{m,p}}{dz} \Big|_{z=\pm \frac{L}{2}} = \mp K'_{m,p} [T_{m,p}(\pm L/2) - T_{R/L}], \quad (17)$$

The solution to Eq. (16) and Eq. (17) yields the magnon-phonon temperature difference $\Delta T_{mp}(z) = T_m(z) - T_p(z)$:

$$\Delta T_{mp}(z) = \frac{K_T (K'_p K_m - K'_m K_p) \sinh \frac{z}{\lambda} \Delta T}{\frac{1}{\lambda} K_m K_p (K'_T L + 2K_T) \cosh \frac{L}{2\lambda} + (2K'_m K_p^2 + 2K'_p K_m^2 + K'_p K'_m L K_T) \sinh \frac{L}{2\lambda}} \equiv \eta \frac{\sinh \frac{z}{\lambda}}{\sinh \frac{L}{2\lambda}} \Delta T \quad (18)$$

with $\Delta T = T_L - T_R$ and

$$\lambda^2 = \frac{C_p + C_m}{C_p C_m} \frac{K_p K_m}{K_p + K_m} \tau_{mp} \approx \frac{K_m}{C_m} \tau_{mp}, \quad (19)$$

where the approximation applies when $C_p \gg C_m$ and $K_p \gg K_m$. Eq. (18) shows that the deviation of the magnon temperature from the lattice (phonon) temperature is proportional to the applied temperature bias and decays to zero far from the boundaries with characteristic (magnon diffusion) length λ .

We use the diffusion limited magnon thermal conductivity and specific heat calculated by a simple kinetic theory (assuming $\hbar\omega_0 \ll k_B T$):¹²

$$C_m = \frac{15\zeta(\frac{5}{2})}{32} \sqrt{\frac{k_B^5 T^3}{\pi^3 D^3}} \quad \text{and} \quad K_m = \frac{35\zeta(\frac{7}{2})}{16} \sqrt{\frac{k_B^7 T^5}{\pi^3 D}} \frac{\tau_m}{\hbar^2}$$

with τ_m the magnon scattering time. Using these expressions in the approximate form of Eq. (19) we obtain:

$$\lambda^2 = \frac{14\zeta(7/2)}{3\zeta(5/2)} \frac{D k_B T}{\hbar^2} \tau_m \tau_{mp}. \quad (20)$$

In Appendix D, we estimate $\tau_{mp} \simeq 1/(2\alpha\omega_0)$ for ferromagnetic insulators, assuming that magnetic damping α is caused by magnon-phonon scattering. It is difficult to estimate or measure τ_m , and the values quoted in the literatures ranges from 10^{-9} s to 10^{-7} s, depending on both material and temperature.^{7,13} At present we cannot predict how λ varies with temperature: Eq. (20) seems to increase with temperature, but the relaxation times likely decrease with T.

When $K'_m \rightarrow 0$ and $K'_p \rightarrow \infty$, *i.e.* the boundary is thermally insulated for magnons and has zero thermal resistivity for phonons, the prefactor η in Eq. (18) reduces to SW's result:⁶

$$\eta = \frac{K_T}{\frac{L}{\lambda} K_p \coth \frac{L}{2\lambda} + 2K_m} \approx \frac{1}{\frac{L}{\lambda} \coth \frac{L}{2\lambda}}, \quad (21)$$

where the approximation is valid when $K_p \gg K_m$. ΔT_{mp} is obviously maximal in this limit.

The discussion in this section also applies to ferromagnetic metals when the electron-phonon relaxation is much faster than the magnon-phonon relaxation. The electron and phonon subsystem are then thermalized with each other and can be treated as one subsystem. In this case, we may replace $K_p \rightarrow K_{pe} = K_p + K_e$ and

$$\frac{C_p C_m}{C_p + C_m} \frac{1}{\tau_{mp}} \rightarrow \frac{C_p C_m}{C_p + C_m} \frac{1}{\tau_{mp}} + \frac{C_e C_m}{C_e + C_m} \frac{1}{\tau_{me}}. \quad (22)$$

IV. HALL VOLTAGE

In Uchida *et al.*'s experiment (Ref. 2), a Pt contact is attached on top of a Py film (see Fig. 1) to detect the spin current signals by the inverse spin Hall effect. A spin current polarized in the \hat{z} -direction that flows into the contact in the \hat{y} -direction is converted into an electric Hall current I_c and thus a Hall voltage $V_H = I_c R$ in the \hat{x} -direction.

	YIG	Py	Unit
γ	1.76×10^{11}	1.76×10^{11}	1/T·s
$4\pi M_s$	$^a 1.4 \times 10^5$	$^f 8.0 \times 10^5$	A/m
D	$^b 1.55 \times 10^{-38}$	$^f 7.6 \times 10^{-39}$	J·m ²
α	$^a 5 \times 10^{-5}$	$^g 0.01$	—
ω_0	$^a 10$	$^g 20$	GHz
τ_{mp}	$^{c,d} 10^{-6}$	$^d 10^{-7}$ (Ni)	s
τ_m	$^{c,e} 10^{-9 \sim 7}$	$^h 10^{-9}$	s
$\frac{g_r}{A}$	$^a 10^{15 \sim 16}$	$^i 10^{18}$	1/m ²
$V_a^{1/3}$	5.4	3.8	nm
η	0.4 - 0.5	0.27	—
λ (th)	4.7 - 47	0.3	mm
λ (exp)	$^a 6.7$	$^k 4.0$	mm
ξ (th)	0.38 - 3.8	130	$\mu\text{V/K}$
ξ (exp)	$^a 0.16$	$^k 0.25$	$\mu\text{V/K}$

TABLE I. Parameters for YIG and Py (at $T = 300\text{K}$ if not specified, $LT \approx 10\text{ K}$). ^aRef. 17, ^bRef. 18, ^cRef. 13, ^dRef. 16, ^eRef. 7, ^fRef. 19 (D is derived from $A_{\text{ex}} = 13\text{ pJ/m}$), ^gRef. 20, ^hRef. 21, ⁱRef. 22, ^jRef. 2.

Quantity	Values	Reference
θ_H	0.0037	4
ρ	$0.91\ \mu\Omega\cdot\text{m}$	2
$l \times w \times h$	$4\text{ mm} \times 0.1\text{ mm} \times 15\text{ nm}$	2

TABLE II. Parameters for Pt contact.

For the setup shown in Fig. 1 we assume that the Pt contact is small enough to not disturb the system, which is valid when the heat flowing into Pt is much less than the heat exchange between the magnons and phonons or

$$K'_m \Delta T_{mp}(z)(l \times w) \ll \frac{C_p C_m}{C_T} \frac{1}{\tau_{mp}} \Delta T_{mp}(z)(l \times w \times d),$$

which is well satisfied when $d \gg 1\text{ nm}$ for both YIG and Py at low temperatures.

From Eq. (18), we see that at the position below the contact ($z = z_c$) the magnon temperature deviates from the lattice (and electron) temperatures by $T_F^m - T_F^p = \Delta T_{mp}(z_c)$. If we assume that the contact is at thermal equilibrium with the lattice (and electrons) in the F film underneath, *i.e.* $T_c^e = T_c^p = T_F^p(z_c)$, then a temperature difference between the magnons in F and the electrons in Pt exists: $T_F^m(z_c) - T_c^e = \Delta T_{mp}(z_c)$. Therefore, by Eq. (12), a DC spin-pumping current $\langle I_z \rangle$ from F to Pt is driven by this temperature difference, which gives rise to a DC Hall current in the Pt contact (see Fig. 1):

$$j_c \hat{\mathbf{x}} = \theta_H \frac{2e}{\hbar} \frac{\langle I_z \rangle}{A} \hat{\mathbf{z}} \times \hat{\mathbf{y}}, \quad (23)$$

where θ_H is the Hall angle. In Eq. (23) we disregarded the spin diffusion backflow and finite thickness corrections to

the Hall effect, which is reasonable when thickness h is comparable to the spin diffusion length l_{sd} .

According to Eq. (12), the thermally driven spin pumping current can flow from F to Pt:

$$\langle I_z \rangle = L'_s [T_m(z_c) - T_c] = L'_s [T_m(z_c) - T_p(z_c)]. \quad (24)$$

Making use of Eq. (18), the electric voltage over the two transverse ends of the Pt contact separated by distance l is $V_H(z_c) = \rho l j_c(z_c)$:

$$V_H = \frac{\eta \theta_H \rho l g_r \gamma e k_B}{\pi M_s V_a A} \frac{\sinh \frac{z_c}{\lambda}}{\sinh \frac{l}{2\lambda}} \Delta T \equiv \xi \frac{\sinh \frac{z_c}{\lambda}}{\sinh \frac{l}{2\lambda}} \Delta T, \quad (25)$$

Using the numbers in Table I and Table II and a value of $\lambda \simeq 7\text{ mm}$ that reflects the low magnetization damping in YIG, we have $\eta \simeq 0.47$ from Eq. (21), and $\xi \simeq 0.38 \sim 3.8\ \mu\text{V/K}$ from Eq. (25) for YIG for $g_r/A \simeq 10^{15 \sim 16}/\text{m}^2$, which is consistent with the experiments by Uchida *et al.* (Ref. 18). For Py, we estimate $\xi \simeq 130\ \mu\text{V/K}$, which is almost three orders of magnitude larger than the experimental value of $0.25\ \mu\text{V/K}$ given in Ref. 2.

The crucial length scale λ is determined by two thermalization times: the magnon-magnon thermalization time τ_m and the magnon-phonon thermalization time τ_{mp} as shown in Eq. (20). Knowledge of these two times is essential in estimating λ . The quoted values of $\tau_{m,mp}$ are rough order of magnitude estimates at low temperatures. Yet, in order to completely pin down the value of λ for this material, a more accurate determination of $\tau_{m,mp}$ and K_m, C_m as a function of temperature by both theory and experiments is required. As seen in Eq. (25), the spatial variation of the Hall voltage over the F strip is determined by the magnon-phonon temperature difference profile as calculated in the previous section. From Eq. (20) and the parameters for YIG in Table I (where the values of τ_m and τ_{mp} are very uncertain), we estimate $\lambda \simeq 4.7 \sim 47\text{ mm}$, which is again consistent with the experimental value of $\lambda \simeq 6.7\text{ mm}$. For Py, we estimate $\lambda \simeq 0.3\text{ mm}$ (using the τ_{mp} value for Ni instead of Py), which is about one order of magnitude smaller than its measured value.

V. DISCUSSION & CONCLUSION

A magnon-phonon temperature difference drives a DC spin current, which can be detected by the inverse spin Hall effect or other techniques. This effect can, *vice versa*, be used to measure the magnon-phonon temperature difference. Because the spatial dependence of this effect relies on various thermalization times between quasiparticles, which are usually difficult to measure or calculate, this effect also accesses these thermalization times. On a basic level, we predict that the spin Seebeck effect is caused by the non-equilibrium between magnon and phonon systems that is excited by a temperature basis over a ferromagnet. Since the inverse spin Hall effect

only provides indirect evidence, it would be interesting to measure the presumed magnon-phonon temperature difference profile by other means. Such measurements would also give insight into relaxation times that are difficult to obtain otherwise.

In principle, the theory holds for both ferromagnetic insulators and metals. However, as shown above, the agreement between the theory and experiments is reasonably good for ferromagnetic insulator YIG, but the theory fails for ferromagnetic metal Py, which underestimates the length scale λ and overestimates the magnitude ξ . This might be because of several reasons: (i) we have completely ignored the short-circuiting effect of the metallic Py, to which the inverse spin Hall current leaks, (ii) the lack of reliable information about relaxation times $\tau_{mp,m}$ for Py could cause the difference in λ , (iii) the complication due to the existence of conduction electrons in ferromagnetic metals.

In conclusion, we propose a mechanism for the spin Seebeck effect based on the combination of: (i) the inverse spin Hall effect, which converts the spin current into an electrical voltage, (ii) thermally activated spin pumping at the F|N interface driven by the phonon-magnon temperature difference, and (iii) the phonon-magnon temperature difference profile induced by the temperature bias applied over a ferromagnetic film. Effect (ii) also introduces an additional magnon contributed thermal conductivity of F|N interfaces. The theory holds for both ferromagnetic metals and insulators. The agreement between experiments and theory is satisfactory for insulating ferromagnet. The magnitude and the spatial length scale for YIG is predicted to be in microvolt and millimeter range. The lack of agreement for both the length scale and the magnitude of the spin Seebeck effect for permalloy remains to be explained.

ACKNOWLEDGMENT

This work has been supported by EC Contract IST-033749 ‘‘DynaMax’’, a Grant for Industrial Technology Research from NEDO, Japan, and National Natural Science Foundation of China (Grand No. 10944004). J. X. and G. B. acknowledge the hospitality of the Maekawa Group at the IMR, Sendai.

Appendix A: Integral

Here we evaluate the frequency integral in Eq. (12). To this end, we need to reintroduce the time dependence and then take the limit $t \rightarrow 0$. When $t > 0$, the integral in Eq. (10b) can be calculated using contour integration (real axis + semi-circle in the lower plane so that $e^{-i\omega t} \rightarrow 0$, where the integral over the semi-circle

vanishes by *Jordan’s Lemma*):

$$\int \chi e^{-i\omega t} \frac{d\omega}{2\pi} = -i \operatorname{Im} \left[\frac{e^{-i\omega_- t}}{1 - i\alpha} (\hat{1} - \hat{\sigma}_y) \right] \Theta(t). \quad (\text{A1})$$

The minus sign comes from the counter-clockwise contour, and $\Theta(t)$ is the Heaviside step function, which vanishes when $t < 0$ and is unity otherwise. This integral is discontinuous at $t = 0$, therefore the value at $t = 0$ is given by the average of the values at $t = 0^\pm$:

$$\int \chi e^{-i\omega 0} \frac{d\omega}{2\pi} = \frac{1}{2} \frac{1}{1 + \alpha^2} \begin{pmatrix} \alpha & 1 \\ -1 & \alpha \end{pmatrix}. \quad (\text{A2})$$

Appendix B: Spin-mixing conductance for F|N interface

In this Appendix, we use a simple parabolic band model to estimate the spin pumping at an F|N interface, where F can be a conductor or an insulator. The Fermi energy in N is E_F , and the bottom of the conduction band for spin up and spin down electrons in F are at $E_F + U_0$ and $E_F + U_0 + \Delta$, respectively, where U_0 is the bottom of the majority band and Δ is the exchange splitting. The reflection coefficient for an electron spin σ (\uparrow or \downarrow) from N at the Fermi energy reads

$$r_\sigma(k) = \frac{k - k_\sigma}{k + k_\sigma} \quad (\text{B1})$$

where $k = \sqrt{2m_0 E_F / \hbar^2 - q^2}$ is the longitudinal wave-vector in N (q is the transverse wave-vector). $k_\uparrow = \sqrt{2m_\uparrow (E_F - U_0) / \hbar^2 - q^2}$ and $k_\downarrow = \sqrt{2m_\downarrow (E_F - U_0 - \Delta) / \hbar^2 - q^2}$ are the longitudinal wave-vectors (or imaginary decay constants) in F for both spins. m_0 is the effective mass in N and m_σ is the effective mass for spin σ in F. The mixing conductance reads

$$g_{\text{mix}} = \frac{A}{4\pi^2} \int (1 - r_\uparrow r_\downarrow^*) d^2 \mathbf{q} = g_r + i g_i. \quad (\text{B2})$$

We evaluate Eq. (B2) with $m_0 = m_\sigma$ having the free electron mass, $E_F = 2.5$ eV, $U_0 = 0 - 4$ eV.²⁴ A plot of the mixing conductance is shown in Fig. 3 for $\Delta = 0.3, 0.6, 0.9$ eV. $U_0 = 0$ corresponds to a ferromagnetic metal (with majority band matching the N electronic structure), and $U_0 \geq E_F = 2.5$ eV corresponds to a ferromagnetic insulator (with $|r_\sigma| = 1$ for both spin types).

Appendix C: Magnetization correlation for macroscopic samples

The dynamics of \mathbf{m} is governed by the LLG equation:

$$\dot{\mathbf{m}}(\mathbf{r}, t) = -\gamma \mathbf{m}(\mathbf{r}, t) \times \mathbf{H}_{\text{eff}} + \alpha \mathbf{m}(\mathbf{r}, t) \times \dot{\mathbf{m}}(\mathbf{r}, t), \quad (\text{C1})$$

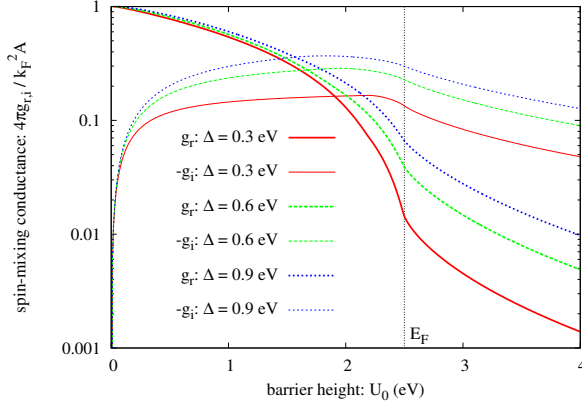


FIG. 3. (Color online) $g_{r,i}$ vs. U_0 in logscale for different Δ values. Curves starting with values close to unity give the real part g_r , and curves starting from very low values display the imaginary part $-g_i$. The vertical axis is in units of the Sharvin conductance.

where $\mathbf{H}_{\text{eff}} = \mathbf{H}_0 + (D/\gamma\hbar)\nabla^2\mathbf{m}(\mathbf{r}, t) + \mathbf{h}(\mathbf{r}, t)$ is the total effective magnetic field with: (i) the external field plus the uniaxial anisotropy field $\mathbf{H}_0 = H_0\hat{\mathbf{z}} = (\omega_0/\gamma)\hat{\mathbf{z}}$, (ii) the exchange field $(D/\gamma\hbar)\nabla^2\mathbf{m}$ due to spatial variation of magnetization, and (iii) the thermal random fields $\mathbf{h}(\mathbf{r}, t)$.

We define Fourier transforms:

$$\tilde{g}(\mathbf{k}, \omega) = \int d\mathbf{r} e^{i\mathbf{k}\cdot\mathbf{r}} \int dt e^{i\omega t} g(\mathbf{r}, t) \quad (\text{C2})$$

$$g(\mathbf{r}, t) = \frac{1}{V} \sum_{m,n,l} e^{-i\mathbf{k}\cdot\mathbf{r}} \int \frac{d\omega}{2\pi} e^{-i\omega t} \tilde{g}(\mathbf{k}, \omega) \quad (\text{C3})$$

where $\mathbf{k} = 2\pi(m/L, n/W, l/H)$ and L, W, H are the length, width, and height of the ferromagnetic film. Near thermal equilibrium, $m_\perp \ll 1$ (and so $m_z \simeq 1$), we may linearize the LLG equation. After Fourier transformation, the linearized LLG equation becomes $\tilde{m}_i(\mathbf{k}, \omega) = \sum_j \chi_{ij}(\mathbf{k}, \omega) \tilde{h}_j(\mathbf{k}, \omega)$ with $i, j = x, y$, and

$$\chi = -\frac{1/(1+\alpha^2)}{(\omega - \omega_{\mathbf{k}}^+)(\omega - \omega_{\mathbf{k}}^-)} \begin{pmatrix} \omega_{\mathbf{k}} - i\alpha\omega & -i\omega \\ i\omega & \omega_{\mathbf{k}} - i\alpha\omega \end{pmatrix} \quad (\text{C4})$$

with $\hbar\omega_{\mathbf{k}} = \hbar\omega_0 + D|\mathbf{k}|^2$ and $\omega_{\mathbf{k}}^\pm = \pm\omega_{\mathbf{k}}/(1 \pm i\alpha)$.

The spectrum of random motion in the linear response regime $x_i = \sum_j \chi_{ij} f_j$ with “current” x and random force f (x and f are chosen such that xf is in the units of energy) is comprehensively studied in Ref. 25. In our problem, $f \rightarrow \gamma\hbar$, $x \rightarrow (M_s/\gamma)m$, $\chi \rightarrow (M_s/\gamma)\chi$, the autocorrelation of the magnetization then becomes ($\zeta = \mathbf{r}_1 - \mathbf{r}_2$, $\tau = t_1 - t_2$)

$$\langle m_i(\zeta, \tau) m_j(0, 0) \rangle = \frac{2\gamma k_B T}{M_s V} \times \sum_{\mathbf{k}} e^{-i\mathbf{k}\cdot\zeta} \int \frac{d\omega}{2\pi} e^{-i\omega\tau} \frac{\chi_{ij} - \chi_{ji}^*}{i\omega} \frac{\hbar|\omega|/k_B T}{e^{\hbar|\omega|/k_B T} - 1}, \quad (\text{C5})$$

from which $\langle \dot{m}_i(\zeta, \tau) m_j(0, 0) \rangle$ can be calculated by taking derivative over τ .

The limit $\zeta = 0$ and $\tau = 0$ can be obtained for three-dimensional systems by replacing the sum over \mathbf{k} by an integral $V^{-1} \sum_{\mathbf{k}} \rightarrow \int d^3\mathbf{k}/(2\pi)^3$ in Eq. (C5):

$$\langle m_i(0, 0) m_j(0, 0) \rangle = Z^{\frac{3}{2}} \frac{\gamma\hbar}{M_s} \left(\frac{k_B T}{4\pi D} \right)^{\frac{3}{2}} \delta_{ij}, \quad (\text{C6})$$

$$\langle \dot{m}_i(0, 0) m_j(0, 0) \rangle = \frac{3Z^{\frac{5}{2}} \gamma k_B T}{2M_s} \left(\frac{k_B T}{4\pi D} \right)^{\frac{3}{2}} \begin{pmatrix} -\alpha & -1 \\ 1 & -\alpha \end{pmatrix}_{ij}, \quad (\text{C7})$$

where Z is the Zeta function.

Appendix D: Relation between α and τ_{mp}

Here we derive a relationship between the magnetic damping constant α and the magnon-phonon thermalization time τ_{mp} . When the magnon and phonon temperatures are T_m and T_p , the magnon-phonon relaxation time is phenomenologically defined by:⁶

$$\frac{d}{dt}(T_p - T_m) = -\frac{T_p - T_m}{\tau_{mp}}. \quad (\text{D1})$$

If the phonon system is attached to a huge reservoir (substrate) such that its temperature T_p is fixed ($dT_p/dt = 0$), Eq. (D1) becomes

$$\frac{dT_m}{dt} \simeq -\frac{T_m - T_p}{\tau_{mp}}. \quad (\text{D2})$$

In metals we should consider three subsystems (magnon, phonon, electron) leading to

$$\frac{dT_s}{dt} = -\sum_t k_{st}(T_s - T_t), \quad (\text{D3})$$

with $s, t = m, p, e$ for magnon, phonon, and electron. The coupling strength $k_{st} = \tau_{st}^{-1} C_t / (C_s + C_t)$ with the s - t relaxation time τ_{st} and the specific heat C_s . When the magnon specific heat is much less than that of phonons and electrons ($C_m \ll C_p, C_e$)

$$\frac{dT_m}{dt} \simeq -\frac{T_m - T_p}{\tau_{mp}} - \frac{T_m - T_e}{\tau_{me}}. \quad (\text{D4})$$

We may parameterize the magnon temperature by the thermal suppression of the average magnetization:

$$H_{\text{eff}} M_s V (1 - \langle m_z \rangle) = k_B T_m, \quad (\text{D5})$$

where H_{eff} points in the $\hat{\mathbf{z}}$ -direction. The LLG equation provides us with the information about m_z :

$$\dot{\mathbf{m}} = -\gamma \mathbf{m} \times (\mathbf{H}_{\text{eff}} + \mathbf{h}) + \alpha \mathbf{m} \times \dot{\mathbf{m}}, \quad (\text{D6})$$

where the random thermal field $\mathbf{h} = \mathbf{h}_p + \mathbf{h}_e$ from the lattice and electrons are determined by the phonon/electron temperature:

$$\langle \gamma h_{p/e}^i(t) \gamma h_{p/e}^j(0) \rangle = \frac{2\gamma \alpha_{p/e} k_B T_{p/e}}{M_s V} \quad (\text{D7})$$

$$-\frac{k_B}{H_{\text{eff}} M_s V} \frac{dT_m}{dt} = \langle \dot{m}_z \rangle = \langle m_y \gamma h_x - m_x \gamma h_y \rangle + \alpha \langle m_x \dot{m}_y - m_y \dot{m}_x \rangle = \frac{1}{1 + \alpha^2} \frac{2\gamma k_B (\alpha T_m - \alpha_p T_p - \alpha_e T_e)}{M_s V}, \quad (\text{D8})$$

or

$$\frac{dT_m}{dt} = -\frac{2\omega_0}{1 + \alpha^2} (\alpha T_m - \alpha_p T_p - \alpha_e T_e), \quad (\text{D9})$$

with $\omega_0 = \gamma H_{\text{eff}}$. Comparing Eq. (D9) with Eq. (D4), we find

$$2\alpha\omega_0 \simeq \frac{2\alpha\omega_0}{1 + \alpha^2} = \frac{2\alpha_p\omega_0}{1 + \alpha^2} + \frac{2\alpha_e\omega_0}{1 + \alpha^2} = \frac{1}{\tau_{mp}} + \frac{1}{\tau_{me}}. \quad (\text{D10})$$

with $\alpha_{p/e}$ the magnetic damping caused by scattering with phonons/electrons and $\alpha = \alpha_p + \alpha_e$. Therefore

For the ferromagnetic insulator YIG: $\alpha \simeq 6.7 \times 10^{-5}$ and $\omega_0 \simeq 10$ GHz (Ref. 17), thus $\tau_{mp} = 1/2\alpha\omega_0 \simeq 10^{-6}$ s, which agrees with $\tau_{mp} \simeq 10^{-6}$ s in Ref. 6.

The estimate above relies on the macrospin approximation. Considering magnons from all \mathbf{k} adds a prefactor of order of unity.

-
- ¹ Spin Caloritronics, Special Issue of Sol. Stat. Commun. (G.E.W. Bauer, A.H. MacDonald, and S. Maekawa, eds), **150**, 459 (2010).
 - ² K. Uchida, S. Takahashi, K. Harii, J. Ieda, W. Koshibae, K. Ando, S. Maekawa, and E. Saitoh, Nature **455**, 778 (2008); Sol. Stat. Commun. **150**, 524 (2010).
 - ³ S. O. Valenzuela and M. Tinkham, Nature **442**, 176 (2006).
 - ⁴ T. Kimura, Y. Otani, T. Sato, S. Takahashi, and S. Maekawa, Phys. Rev. Lett. **98**, 156601 (2007).
 - ⁵ M. Hatami, G. E. W. Bauer, S. Takahashi, and S. Maekawa, Sol. Stat. Commun. **150**, 480 (2010).
 - ⁶ D. J. Sanders and D. Walton, Phys. Rev. B **15**, 1489 (1977).
 - ⁷ C. Kittel and E. Abrahams, Rev. Mod. Phys. **25**, 233 (1953).
 - ⁸ E. Beaurepaire, J. Merle, A. Daunois, and J. Bigot, Phys. Rev. Lett. **76**, 4250 (1996).
 - ⁹ Y. Tserkovnyak, A. Brataas, and G. E. W. Bauer, Phys. Rev. Lett. **88**, 117601 (2002).
 - ¹⁰ J. Foros, A. Brataas, Y. Tserkovnyak, and G. E. W. Bauer, Phys. Rev. Lett. **95**, 016601 (2005).
 - ¹¹ J. Xiao, G. E. W. Bauer, S. Maekawa, and A. Brataas, Phys. Rev. B **79**, 174415 (2009).
 - ¹² W. B. Yelon and L. Berger, Phys. Rev. B **6**, 1974 (1972).
 - ¹³ S. O. Demokritov, V. E. Demidov, O. Dzyapko, G. A. Melkov, A. A. Serga, B. Hillebrands, and A. N. Slavin, Nature **443**, 430 (2006).
 - ¹⁴ http://www.isowave.com/pdf/materials/Yttrium_Iron_Garnet.pdf.
 - ¹⁵ S. S. Shinozaki, Phys. Rev. **122**, 388 (1961).
 - ¹⁶ E. G. Spencer and R. C. LeCraw, Phys. Rev. Lett. **4**, 130 (1960).
 - ¹⁷ Y. Kajiwara, K. Harii, S. Takahashi, J. Ohe, K. Uchida, M. Mizuguchi, H. Umezawa, H. Kawai, K. Ando, K. Takanashi, S. Maekawa, and E. Saitoh, Nature **464**, 262 (2010).
 - ¹⁸ K. Uchida, J. Xiao, H. Adachi, J. Ohe, S. Takahashi, J. Ieda, T. Ota, Y. Kajiwara, H. Umezawa, H. Kawai, G. E. W. Bauer, S. Maekawa, E. Saitoh, Nature Materials (in press).
 - ¹⁹ P. E. Roy, J. H. Lee, T. Trypiniotis, D. Anderson, G. A. C. Jones, D. Tse, and C. H. W. Barnes, Phys. Rev. B **79**, 060407 (2009).
 - ²⁰ V. Vlaminck and M. Bailleul, Science **322**, 410 (2008).
 - ²¹ Y. Hsu and L. Berger, Phys. Rev. B **14**, 4059 (1976).
 - ²² A. Brataas, G. E. W. Bauer, and P. J. Kelly, Physics Reports **427**, 157 (2006).
 - ²³ S. Takahashi and S. Maekawa, Science and Technology of Advanced Materials **9**, 014105 (2008).
 - ²⁴ D. Jin, Y. Ren, Z. zhong Li, M. wen Xiao, G. Jin, and A. Hu, in J. Appl. Phys. **99**, 08T304-3 (2006).
 - ²⁵ L. D. Landau, E. M. Lifsic, L. P. Pitaevskii, J. Sykes, and M. J. Kearsley, *Statistical physics Vol. 9* (Butterworth-Heinemann, 1980).